A mathematical model of dynamics of cell populations in squamous epithelium after irradiation

Martín Parga-Pazos[1,2], Óscar López Pouso[1,2], John D. Fenwick[3,4], Juan Pardo-Montero[1,5,*]

1. Group of Medical Physics and Biomathematics, Instituto de Investigación Sanitaria de Santiago (IDIS), Santiago de Compostela, Spain.

2. Department of Applied Mathematics, Universidade de Santiago de Compostela, Santiago de Compostela, Spain.

3. Department of Molecular and Clinical Cancer Medicine, Institute of Translational Medicine, University of Liverpool, Liverpool, United Kingdom.

4. Department of Physics, Clatterbridge Cancer Centre, Clatterbridge Road, Wirral, United Kingdom.

5. Department of Medical Physics, Complexo Hospitalario Universitario de Santiago de Compostela, Spain.

* Corresponding author

Running title: Model of cell populations in epithelium after irradiation

Corresponding authors: Juan Pardo-Montero, Instituto de Investigación Sanitaria de Santiago (IDIS), Servizo de Radiofísica e Protección Radiolóxica, Hospital Clínico Universitario de Santiago, Trav. Choupana s/n, 15706, Santiago de Compostela; Phone: +34 981950969; E-mail: juan.pardo.montero@sergas.es

Funding details: This project was funded by Instituto de Salud Carlos III (ISCIII) through research grants PI17/01428 and DTS17/00123 (FEDER co-funding). J.P-M. is supported by ISCIII through a Miguel Servet II grant (CPII17/00028, FEDER co-funding). O.L.P. is partially supported by FEDER and Xunta de Galicia (GRC2013-014), and by the Spanish Ministry of Science, Innovation and Universities (MTM2017-86459-R).

Biographical note

Martín Parga-Pazos carried on his MSc thesis in the Group of Medical Physics and Biomathematics at the Health Research Institute of Santiago, working on dynamics of cell populations in squamous epithelium after radiotherapy. He is currently a PhD student at CIC bioGUNE.

Óscar López Pouso is a faculty member in the Department of Applied Mathematics at the University of Santiago de Compostela. His areas of interest are the analysis and numerical resolution of mathematical models for applied sciences and biomedicine.

John D. Fenwick is a senior lecturer in the Institute of Translational Medicine at the University of Liverpool, and honorary consultant clinical scientist at Clatterbridge Cancer Centre, with research interests in radiotherapy and imaging physics.

Juan Pardo-Montero is a "Miguel Servet" scientist at the Health Research Institute of Santiago (Group of Medical Physics and Biomathematics). His current research is focused on biomathematical models in radiotherapy and oncology, and radiation dosimetry.

Abstract

Purpose: To develop multi-compartment mechanistic models of dynamics of stem and functional cell populations in epithelium after irradiation.

Methods and materials: We present two models, with three (3C) and four (4C) compartments respectively. We use delay differential equations, and include accelerated proliferation, loss of division asymmetry, progressive death of abortive stem cells, and turnover of functional cells. The models are used to fit experimental data on the variations of the number of cells in mice mucosa after irradiation with 13 Gy and 20 Gy. Akaike information criteria (AIC) was used to evaluate the performance of each model.

Results: Both 3C and 4C models provide good fits to experimental data for 13 Gy. Fits for 20 Gy are slightly poorer and may be affected by larger uncertainties and fluctuations of experimental data. Best fits are obtained by imposing constraints on the fitting parameters, so to have values that are within experimental ranges. There is some degeneration in the fits, as different sets of parameters provide similarly good fits.

Conclusions: The models provide good fits to experimental data. Mechanistic approaches like this can facilitate the development of mucositis response models to non-standard schedules/treatment combinations not covered by datasets to which phenomenological models have been fitted. Studying the dynamics of cell populations in multifraction treatments, and finding links with induced toxicity, is the next step of this work.

Keywords: biomathematical model, radiotherapy, mucositis, radiobiology

1. Introduction

Intolerable toxicity in *turnover tissues*, like mucosae or skin, is one of the limiting factors of dose escalation and/or treatment shortening in several cancers, especially those of the head-and-neck (Trotti et al. 2003; Vera-Llonch et al. 2006; Russi et al. 2015; Sroussi et al. 2017). Predicting whether different schedules would lead to tolerable or intolerable toxicity is of paramount importance in order to design unconventional radiotherapy schedules that might increase tumor control. Several mathematical models have been developed to explore this issue. Some of these models aim at separating population-wise tolerable and intolerable schedules, like the early model of Fowler et al. (2003), based on the biologically effective dose (BED), later refined by Fenwick et al. (2008), who provided a modified equation for the BED boundary separating tolerable from intolerable schedules. More recently, Strigari et al. (2012) presented a model based on the Lyman-Kutcher-Burman formulation of Normal Tissue Complication Probability. Other models aim at predicting the probability of toxicity of each treated individual, by including individual dose distributions and other patient data and using dose response models, regression, and machine learning techniques (Bhide et al. 2012; Dean et al. 2016a, Dean et al. 2016b, Dean et al. 2017).

All these models are of a phenomenological nature: they do not explore mechanistically what happens to cell populations in tissues, and how that affects toxicity. Even though such phenomenological models find ample application in the clinic due to their specificity, sensitivity, and simplicity (probably rather more application than any mechanistic complex model would find), it is nonetheless of interest to study this problem from a more mechanistic point of view. Such mechanistic approaches can provide useful insight into the problem and can facilitate the development of phenomenological response models to non-standard schedules/treatment combinations not covered by datasets to which the phenomenological models have been fitted.

There exists a large literature on the effect of radiation and fractionation on the populations of cells

in squamous epithelium (Dörr 1997, Dörr 2009, and references therein). However, the mechanistic modeling of what happens to populations of cells in irradiated squamous epithelium has not been fully addressed. Dörr and Obeyesekere (2001) presented a model of this effect. Hanin and Zaider (2013) presented a mechanistic model of radiation-induced damage to normal tissue and its healing kinetic, which is general and not specifically aimed at squamous epithelium. In this work, we present two variations of a multi-compartmental model of cell populations in irradiated epithelium. The model builds on Dörr and Obeyesekere (2001), and it is based on delay differential equations, with delays accounting for cell replication duration, and transfer between compartments. Fenwick (2006) has used delay differential equations to model mucositis, but did not explore the mechanistic origin of such models. The main biological features sustaining the model are based on the *three A's* of repopulation in irradiated squamous epithelium*:* loss of **A**ssymetry, **A**ccelerated proliferation, and **A**bortive divisions (Dörr 1997). Two models are presented, one of them with three compartments: healthy proliferative cells (S), damaged or abortive proliferative cells (S_A), and differentiated functional stem cells (F); the second one with four compartments: S, S_A, functional cells in the proliferative layer (F_G) and functional cells in the functional layer (F). The second model aims at including the particular structure of epithelium, with an inner germinal layer and an outer functional layer.

We analyze the behavior of both models and use them to fit experimental data of cell densities after irradiation in mouse skin.

2. Methods and Materials

2.1. Overview of the models

Our model will include proliferative stem cells (SC) (please notice that by stem cells we refer to cells with proliferation capacity) and fully differentiated, non proliferative, functional cells (FC). In the equilibrium state, under no perturbations like irradiation, SCs will proliferate asymmetrically,

i.e. each SC division will create one SC and one FC. This asymmetric proliferation will keep the population of SCs constant, in its equilibrium value, and will compensate for the natural loss of FC due to tissue turnover.

At any given time, we assume that a fraction p of SCs is proliferating (the rest being quiescent, in the G0 phase). SC division takes a time, τ, and therefore we will explicitly introduce this delay in our model (hence, the need for delay differential equations). During division, SCs may die (due to fatal damage in their DNA or any other problems activating an apoptotic death). We model this probability of death with the parameter γ_S, which controls an exponential death ($dS/dt=-\gamma_S S$). For healthy SC the probability of dying during division will be small, and so will be this parameter. According to this model, if S SCs start division at time t, $2S \exp(-\gamma_S \tau)$ cells will exit the division cycle at time $t+\tau$, of which a fraction $(1-AF)$ will be SCs and AF will be FCs. If division is fully asymmetrical, $AF=0.5$, it will be ½ SCs and ½ FCs. In Figure 1 we show a scheme of the modeling of the division cycle. This model of cell division and death is based on that presented in Mackey et al. (2003).

Irradiation will damage proliferative SCs, turning them into *abortive* stem cells (ACs). The fraction of SCs turning into ACs by the application of a dose d is given by the surviving fraction (SF), calculated according to the linear-quadratic (LQ) model (Fowler 1989), $SF=\exp(-\alpha d-\beta d^2)$, where α and β are the LQ parameters characterizing cell radiosensitivity, which depend on the amount of DNA damage repair and double-strand breaks misrepair (Sachs et al. 1997). There are concerns about the application of the LQ model to high-doses, due to different effects that can impact surviving fractions, like damage saturation of indirect damage effect associated to vascular damage (Brenner 2008, Kirkpatrick et al. 2008). Alternative models have been proposed for high-doses (Guerrero and Li 2004, Hanin and Zaider 2010). In this work, we will rely on the classical LQ model for the sake of simplicity. ACs will still divide, generating new ACs and FCs. However, they

will have a higher probability of death during division, characterized by a parameter γ_A ($\gamma_A >> \gamma_S$). Therefore, ACs will rapidly disappear, causing a shortage of proliferative cells.

Functional cells are considered non-proliferative, and we also assume they do not die due to the application of radiation. This simplification is based on the higher radiosensitivity of proliferating cells in certain phases of the cycle (Pawlik and Keyomarsi 2004). Functional cells will be lost due to natural turnover. This loss is modeled with an exponential (the rate of loss is proportional to the number of cells), with parameter μ.

The rapid disappearance of proliferative cells after irradiation will cause an important perturbation of the equilibrium state: not only will the number of proliferative cells decrease but so will the number of FCs, as newly generated FCs cannot compensate for turnover. The loss of cells triggers accelerated proliferation and loss of asymmetry (Dörr 1997, Trott 1999, Dörr 2009), aiming at compensating for the loss of functional cells and repopulate the compartment of SCs, therefore restoring the equilibrium of the system (if possible). Accelerated proliferation is modeled as an increase of p, the fraction of proliferating SCs (and ACs). Loss of asymmetry is modeled as a decrease of parameter AF, therefore resulting in the creation of more proliferative cells per division.

In the first model we include the above mentioned three compartments. Squamous epithelium may present a layered structure, with an inner proliferative layer, where stem cells are located and proliferate, and an outer functional layer, composed of functional cells and subject to turnover. This spatial structure is lost in our model (as spatial coordinates are not considered as in any multi-compartmental model). We have extended our initial model to try to accommodate this layered structure. We assume that the proliferative layer contains both SCs and FCs (we refer to FCs in the proliferative layer as PLFs). The functional layer only contains functional cells (which we refer to as FLFs), which have migrated from the proliferative layer where they were created. We consider

SCs to be present only in the proliferative layer. Division of these SCs will create new PLFs, which will then migrate to the functional layer (this migration in modeled with a rate parameter λ and a delay τ_F). Once in the functional layer, FLFs are subject to turnover, as previously described.

In Figures 2 and 3 we present sketches of the 3-compartment (3C) model and the 4-compartment (4C) model, which graphically illustrate the behavior of both models.

2.2. Case 1: 3-compartments (3C) model

The temporal evolution of the three compartments included in Case 1 (stem cells, *S*, abortive stem cells, S_A, and functional cells, *F*) is described by the following equations:

$$\frac{dS(t)}{dt} = \frac{2p(t-\tau)}{\tau} S(t-\tau) e^{-\gamma_S \tau} (1 - AF) - \frac{p(t)}{\tau} S(t) \quad (1)$$

$$\frac{dS_A(t)}{dt} = \frac{2p(t-\tau)}{\tau} S_A(t-\tau) e^{-\gamma_A \tau} (1 - AF) - \frac{p(t)}{\tau} S_A(t) \quad (2)$$

$$\frac{dF(t)}{dt} = \frac{2p(t-\tau)AF}{\tau} [e^{-\gamma_S \tau} S(t-\tau) + e^{-\gamma_A \tau} S_A(t-\tau)] - \mu F(t) \quad (3)$$

In addition, when radiation is delivered there is an instant transfer of a fraction (1-*SF)* of *S* cells to the abortive stem cell compartment, as previously described. In the above set of equations, *AF* is evaluated at *t*-τ, which is not explicitly included in the equation for the sake of simplicity. The factor *p/τ* can be interpreted as a proliferation rate.

A relationship between *p* and the rest of the parameters can be obtained from the equilibrium state condition (denoted by sub-index 0):

$$\frac{dF(t)}{dt} = \frac{1}{\tau} p_0 S_0 e^{-\gamma_s \tau} - \mu F_0 = 0 \;\Rightarrow\; p_0 = \frac{\mu \tau F_0}{S_0 e^{-\gamma_s \tau}} \tag{4}$$

As previously described, the parameters AF and p have a dependence on the number of functional and proliferative cells. It is known that the loss of functional cells triggers accelerated proliferation. In addition, the stem cell compartment will restore itself if damaged (Dörr 1997, Trott 1999). Lacking firm experimental evidence on the functional form of AF and p, we have considered the following simple expressions for these terms:

$$AF(t) = min\left(0.5, \frac{S(t) + S_A(t)}{S_0}\right) \tag{5}$$

$$p(t) = 1 - (1 - p_0)\frac{F(t)}{F_0} \tag{6}$$

The decrease of proliferative cells will result in a decrease of AF and therefore each division will produce on average more proliferative cells (S or S_A). On the other hand, p will increase with decreasing numbers of functional cells, from a value p_0 at equilibrium to approach 1 when the number of functional cells is very low, which will result in almost 100% of S or S_A proliferating.

2.3. Case 2: 4-compartments (4C) model

The temporal evolution of the four compartments included in Case 2 (stem cells, S, abortive stem cells, S_A, functional cells in the proliferative layer, F_G, and functional cells in the functional compartment, F) is described by the following equations:

$$\frac{dS(t)}{dt} = \frac{2p(t-\tau)}{\tau} S(t-\tau) e^{-\gamma_s \tau}(1 - AF) - \frac{p(t)}{\tau} S(t) \tag{7}$$

$$\frac{dS_A(t)}{dt} = \frac{2\,p(t-\tau)}{\tau} S_A(t-\tau) e^{-\gamma_A \tau}(1-AF) - \frac{p(t)}{\tau} S_A(t) \quad (8)$$

$$\frac{dF_G(t)}{dt} = \frac{2\,p(t-\tau)\,AF}{\tau} [e^{-\gamma_S \tau} S(t-\tau) + e^{-\gamma_A \tau} S_A(t-\tau)] - \lambda F_G(t-\tau_F) \quad (9)$$

$$\frac{dF(t)}{dt} = \lambda F_G(t-\tau_F) - \mu F(t) \quad (10)$$

As previously stated, when radiation is delivered there is an instant transfer of a fraction (1-*SF*) of *S* cells to the abortive stem cell compartment, and *AF* is evaluated at time *t*-*τ*. The following relationships can be obtained from the equilibrium state condition:

$$\frac{dF(t)}{dt} = 0 \;\Rightarrow\; \lambda = \frac{\mu F_0}{F_{G,0}} \quad (11)$$

$$\frac{dF_G(t)}{dt} = 0 \;\Rightarrow\; p_0 = \frac{\lambda \tau F_{G,0}}{S_0 e^{-\gamma_S \tau}} = \frac{\mu \tau F_0}{S_0 e^{-\gamma_S \tau}} \quad (12)$$

Again, sub-indices 0 indicate equilibrium populations. We use the same functional form for *AF* and *p* as in equations (5) and (6).

2.4. Experimental results and fits

We have used our models to fit experimental data reported in Dörr and Obeyesekere (2001). In that article, the authors report variations of numbers of cells (cells/mm) with time in the tongue mucosa of mice after irradiation with 13 Gy and 20 Gy. They include densities of cells in the proliferative layer, functional layer, and total. Data were extracted with the graphical software g3data.

2.5. Numerical implementation

The models were implemented in Matlab (The Mathworks, Natwick, MA), and are solved by employing a Euler method (Press et al. 2017), with a time discretization *Δt*, including some particularities, which are described now: Initial values for each compartment are set in such a way

that we are close to an equilibrium solution. Then, the system evolves without any perturbation (irradiation) so as to achieve a real initial equilibrium state (there may be some shift from the initially set initial values, and some oscillation around new equilibrium values, typical of delay differential equations). When the new equilibrium is achieved (defined as a relative moving average varying less than a given ε) these new values are reset as equilibrium values, and we can start the irradiation phase: the abortive compartment is created at the time of dose delivery and filled with a fraction *SF* of *S* cells.

In addition, a simulated annealing method (Press et al. 2017) was implemented to find best fitting parameters. In order to obtain best fitting parameters, the simulated annealing algorithm can stochastically vary the parameters, but such variations are limited to a range of physically and biologically sound parameters, in order to avoid unreasonable good fits. In order to reduce the number of free parameters, we have imposed α/β=10 in the evaluation of surviving fractions with the LQ model, which is a reasonable value for proliferative cells.

In order to fit the experimental data, we have to obtain numbers of cells in the proliferative and functional layers with our model. In addition to the parameters presented in the differential equations showing the dynamical evolution of each model, we need extra parameters to fit the experimental data. Those parameters are: N_T (overall number of cells pre-irradiation), f_S (fraction of stem cells pre-irradiation), and for the 4C model, f_F (fraction of the total number of functional cells that are in the functional compartment pre-irradiation). From these parameters, we can obtain the values of S_0, and F_0 (and $F_{G,0}$ in the 4C model).

We jointly fit data for 13 Gy and 20 Gy, meaning that the same set of fitting parameters are used for both sets of data, but for N_T, f_F, and f_S. The rationale behind this is that the biological parameters (proliferation, turnover, response to radiation) should be the same in both experiments, but the

number of cells in the proliferative and functional compartments is clearly different in the reported experimental data.

We use the weighted sum of squared differences, G, and the Akaike information criterion, AIC, (Akaike 1974; Gordon 2015) to evaluate the goodness of fits with models 3C and 4C:

$$G=\sum_i \left(\frac{d_{\exp,i}- d_{th,i}}{\sigma_{\exp,i}}\right)^2 \quad (13)$$

$$AIC= 2(k+1)+n\log(G/n) \quad (14)$$

where d_{exp} and d_{th} are experimental and theoretical cell densities, respectively, and σ_{exp} are the experimental uncertainties. On the other hand, k is the number of parameters of the model, and n is the sample size. The 3C model has k=9, the 4C-model k=12, and n=64.

3. Results and discussion

In Figures 4 and 5 we show the evolution of densities of cells in the proliferative and functional layers of the skin of mice after irradiation with 13 Gy and 20 Gy, comparing experimental data and best fits obtained with 3C and 4C models, respectively. We present best fits obtained with our SA algorithm, and we also present an uncertainty analysis to illustrate the effect of uncertainties of parameters in the response of the models: to achieve this we performed 1000 simulations that include perturbation of the best fitting parameters, and report best fits ±1 standard deviation (SD). Uncertainties in the parameters are assumed to follow a normal distribution, with standard deviations of 10% of the mean. Combinations of parameters that were unphysical (e.g. values below 0 or above 100%) or lead to divergences were removed.

Both 3C and 4C models provide a good fit of experimental data for irradiation with 13 Gy

(goodness of fit, G=12.4 and 14.2, respectively). Experimental points are generally within the ±1 SD of the uncertainty analysis, showing that this represents an accurate estimation of experimental uncertainties. On the other hand, fits for 20 Gy are poorer (G=29.2 and 22.5 with 3C and 4C models, respectively). The quality of the fits for 20 Gy may be affected by the larger uncertainty of the experimental data (in fact, the uncertainty analysis with standard deviations of 10% of the mean spans over a range much smaller than the experimental uncertainty bars). Also, the large number of cells in both layers post-recovery, around days 13-15, complicates the fit, as this overgrowth is difficult to fit with our models. It is interesting to hypothesize that the overgrowth might be a result of oscillations in the number of cells around the equilibrium populations. Such behavior can appear in models with delays like those presented in this work, but such a regime has not been fully explored due to the lack of enough experimental data to draw conclusions. Interestingly, the 4C model presents a more oscillatory behavior, which may be due to the presence of more compartments and two delays in the system of differential equations.

We should recall that both 13 Gy and 20 Gy population dynamics have been fitted at once, meaning that the same set of parameters was used for both dose levels (but initial densities of cells, as it is obvious in the experimental data that they differ, see section 2.5). If we allow the optimizer to find different parameters to fit each dose level, the quality of the fit greatly improves, especially for 20 Gy. However, this does not seem justified and should not be the way to proceed in our opinion.

AIC values are similar for the 3C model and the 4C model (-7.5 vs. -9.7), with the larger number of parameters of the 4C model canceling out improved G values. In general, these fits are better than those presented in Dörr and Obeyesekere (2001): better for 13 Gy (G≈14 vs. G≈100) and also for 20 Gy (G≈22 vs. G≈38). When using the Akaike methodology, models with differences in AIC below 2 are generally considered to be equally good, while between 2–6 models are rarely dismissed as differences are not considered significative (Symonds and Moussalli (2011)). Therefore, the two

models can be considered as equally good to fit our dataset.

Best fitting parameters are reported in Table 1. They show a low death rate of healthy stem cells ($\gamma_S \sim 10^{-7}$ h^{-1}), and a faster a death rate of abortive stem cells ($\gamma_A \sim 0.05$ h^{-1}) which results in a half-life of approximately one cell division, and less than 10% of damaged cells undergoing 4 divisions (in line with estimations of around 2-3 abortive divisions per damaged stem cell, Dörr 1997). Turnover rates of functional cells are of the order of 0.03 h^{-1}, resulting in half-lifes of functional cells around 24h. The division time is 12 h, which results in around 28% of the stem cells dividing in the steady state ($p_0 \sim 0.28$). Best fits are obtained with α values around 0.05 Gy^{-1}. While this points to highly radio-resistant cells, it is worth noticing that an even lower value of α (0.02 Gy^{-1}) was used in Dörr and Obeyesekere (2001): cells in this experiment seem to be highly radio-resistant indeed, showing only moderate response to 13 and 20 Gy single-fraction doses. Interestingly, if cells present a decrease in relative radiosensitivity with increasing dose, this would result in a low α value when fitting high-dose data to the LQ model.

It is important to notice that our models present some degeneration: increasing values of α (more radio-sensitive cells) and decreasing values of τ lead to fits of similar quality. This degeneration has not been fully investigated, as the best fitting parameters seem to lack biological meaning (for example equally good fits can be obtained with $\alpha = 0.25$ Gy^{-1} and $\tau = 2$ h, but such short division times do not seem plausible).

4. Conclusions

Intolerable toxicities in *turnover tissues*, like mucosa or skin, are limiting toxicities in several cancers. Predicting whether a treatment will cause intolerable toxicity is of paramount importance in order to design optimal radiation treatments. Several phenomenological mathematical models have been developed to explore this issue, and some are used in the clinic. It is nonetheless of

interest to study this problem from a more mechanistic point of view.

In this work, we address the modeling of population dynamics of cells in irradiated squamous epithelium. The multi-compartmental models that we have developed intuitively present the underlying biology in mathematical form, in particular the *three A's* of repopulation in irradiated squamous epithelium. While we refer to our model as mechanistic, it is important to point out that the model here presented uses the LQ model to evaluate surviving fractions of irradiated cells. The LQ model was originally introduced as a phenomenological model, and there has been a long-standing debate on the mechanistic origin of the LQ model (Sachs and Brenner 1998, Zaider 1998), which is still active nowadays (Bodgi and Foray 2016). Also, application of the LQ model to large doses per fraction is questioned, but other approaches like the Linear-Quadratic-Linear (LQL) model (Guerrero and Li 2004) could be easily integrated within this methodology.

The models that we present are deterministic models. The experimental data used for validation include relatively large numbers of cells, but when modeling the dynamics of populations of a few cells, stochastic models may be more appropriate (Hanin 2001, Badry and Leder 2016).

The models were used to fit experimental data of cell population dynamics after single dose irradiation, and we obtained good results. Fits obtained with our model are better than those obtained with a model presented by Dörr and Obeyesekere (2001).

Approaches like the one adopted in this work can provide useful insights into the interpretation and development of phenomenological models of toxicity, if toxicity is mainly due to cell loss in the affected organ (Rutkowska et al 2010). In particular, such mechanistic approaches can facilitate the development of response models to non-standard schedules/treatment combinations not covered by datasets to which the phenomenological models have been fitted, like, for example, unconventional

dose fractionations delivering differing doses per week/day. Unconventional chemo-radiotherapy combinations could also be modeled, provided the cytotoxity of chemotherapy is included in the model. Even though we have only fitted single fraction data, the models can also be used for multi-fraction treatments. Studying the dynamics of a cell population in multifraction treatments, and finding links between such dynamics and induced toxicity, is the next step of this work.

Disclosure of interest: The authors report no conflict of interest.

References

Akaike H. A new look at the statistical model identification. IEEE Transactions on Automatic Control. 1974;19(6): 716-723.

Badry H, Leder K. Optimal treatment and stochastic modeling of heterogeneous tumors. Biol Direct. 2016;11:40

Bhide SA, Gulliford S, Schick U, Miah A, Zaidi S, Newbold K, Nutting CM, Harrington KJ. Dose-response analysis of acute oral mucositis and pharyngeal dysphagia in patients receiving induction chemotherapy followed by concomitant chemo-IMRT for head and neck cancer. Radiother Oncol. 2012;103(1):88-91.

Bodgi L, Foray N. The nucleo-shuttling of the ATM protein as a basis for a novel theory of radiation response: resolution of the linear-quadratic model. Int J Radiat Biol 2016:92;117-131

Brenner DJ. The linear-quadratic model is an appropriate methodology for determining isoeffective doses at large doses per fraction. Semin Radiat Oncol 2008:18;234-9.

Dean JA, Wong KH, Welsh LC, Jones AB, Schick U, Newbold KL, Bhide SA, Harrington KJ, Nutting CM, Gulliford SL. Normal tissue complication probability (NTCP) modelling using spatial dose metrics and machine learning methods for severe acute oral mucositis resulting from head and neck radiotherapy. Radiother Oncol. 2016;120(1):21-27.

Dean JA, Wong KH, Gay H, Welsh LC, Jones AB, Schick U, Oh JH, Apte A, Newbold KL, Bhide SA, Harrington KJ, Deasy JO, Nutting CM, Gulliford SL. Functional data analysis applied to modeling of severe acute mucositis and dysphagia resulting from head and neck radiation therapy. Int J Radiat Oncol Biol Phys. 2016;96(4):820-831.

Dean JA, Welsh LC, Wong KH, Aleksic A, Dunne E, Islam MR, Patel A, Patel P, Petkar I, Phillips I, Sham J, Schick U,

Newbold KL, Bhide SA, Harrington KJ, Nutting CM, Gulliford SL. Normal Tissue Complication Probability (NTCP) modelling of severe acute mucositis using a novel oral mucosal surface organ at risk. Clin Oncol (R Coll Radiol). 2017;29(4):263-273.

Dörr W. Three A's of repopulation during fractionated irradiation of squamous epithelia: Asymmetry loss, Acceleration of stem-cell divisions and Abortive divisions. Int J Radiat Biol. 1997;72(6):635-643

Dörr, W. Time factors in normal tissue responses to irradiation. In: Basic Clinical Radiobiology. (Eds. M. Joiner, A. Vander Kogel), pp.149–157, Hodder Arnold, London, 2009.

Dörr W, Obeyesekere MN. A mathematical model for cell density and proliferation in squamous epithelium after single-dose irradiation. Int J Radiat Biol. 2001;77(4):497-505.

Fenwick JD. Delay differential equations and the dose-time dependence of early radiotherapy reactions. Med Phys. 2006;33(9):3526-3540.

Fenwick JD, Lawrence GP, Malik Z, Nahum AE, Mayles WP. Early mucosal reactions during and after head-and-neck radiotherapy: dependence of treatment tolerance on radiation dose and schedule duration. Int J Radiat Oncol Biol Phys. 2008;71(2):625-634.

Fowler JF. The linear-quadratic formula and progress in fractionated radiotherapy. Br J Radiol. 1989 ;62(740):679-94

Fowler JF, Harari PM, Leborgne F, Leborgne JH. Acute radiation reactions in oral and pharyngeal mucosa: tolerable levels in altered fractionation schedules. Radiother Oncol. 2003;69(2):161-168.

Gordon RA. Regression Analysis for the Social Sciences, Routledge 2015.

Guerrero M, Li XA. Extending the linear- quadratic model for large fraction doses pertinent to stereotactic radiotherapy. Phys Med Biol 2004;49:4825-4835.

Hanin LG. Iterated birth and death process as a model of radiation cell survival. Math Biosci. 2001;169:89-107.

Hanin LG, Zaider M. Cell-survival probability at large doses: an alternative to the linear-quadratic model. Phys Med Biol. 2010;55(16):4687-7702.

Hanin L, Zaider M. A mechanistic description of radiation-induced damage to normal tissue and its healing kinetics.

Phys Med Biol. 2013;58:825-839.

Kirkpatrick JP, Meyer JJ, Marks LB. The linear-quadratic model is inappropriate to model high dose per fraction effects in radiosurgery. Semin Radiat Oncol 2008:18;240-3.

Mackey MC, Haurie C, Bélair J. Cell replication and control. In Non linear dynamics in physiology and medicine (Eds. A. Beuter, L Glass, MC Mackey, MS Titcombe), pp 233-269, Springer 2003.

Pawlik TM, Keyomarsi K. Role of cell cycle in mediating sensitivity to radiotherapy. Int J Radiat Oncol Biol Phys. 2004;59(4):928-42.

Press WH, Teukolsky SA, Vetterling WT, Flannery BP. Numerical Recipes: The Art of Scientific Computing, Cambridge University Press 2007.

Rutkowska E, Baker C, Nahum A. Mechanistic simulation of normal-tissue damage in radiotherapy - implications for dose-volume analyses. Phys Med Biol 2010;55:2121-36.

Russi EG, Moretto F, Rampino M, Benasso M, Bacigalupo A, De Sanctis V, Numico G, Bossi P, Buglione M, Lombardo A, Airoldi M, Merlano MC, Licitra L, Denaro N, Pergolizzi S, Pinto C, Bensadoun RJ, Girolomoni G, Langendijk JA. Acute skin toxicity management in head and neck cancer patients treated with radiotherapy and chemotherapy or EGFR inhibitors: Literature review and consensus. Crit Rev Oncol Hematol. 2015;96(1):167-182.

Sachs RK, Hahnfeld P, Brenner DJ. The link between low-LET dose-response relations and the underlying kinetics of damage production/repair/misrepair. Int J Radiat Biol 1997;72:351-374

Sachs RK, Brenner DJ. The mechanistic basis of the linear-quadratic formalism. Med Phys 1998:25;2071-2072

Sroussi HY, Epstein JB, Bensadoun RJ, Saunders DP, Lalla RV, Migliorati CA, Heaivilin N, Zumsteg ZS. Common oral complications of head and neck cancer radiation therapy: mucositis, infections, saliva change, fibrosis, sensory dysfunctions, dental caries, periodontal disease, and osteoradionecrosis. Cancer Med. 2017;6(12):2918-2931.

Strigari L, Pedicini P, D'Andrea M, Pinnarò P, Marucci L, Giordano C, Benassi M. A new model for predicting acute mucosal toxicity in head-and-neck cancer patients undergoing radiotherapy with altered schedules. Int J Radiat Oncol Biol Phys. 2012;83(5):e697-702.

Symonds MR, Moussalli A. A brief guide to model selection, multimodel inference and model averaging in behavioural

ecology using Akaike's information criterion. Behav Ecol Sociobiol 2011;65(1):13-21.

Trott KR. The mechanisms of acceleration of repopulation in squamous epithelia during daily irradiation. Acta Oncologica. 1999;38:153-157

Trotti A, Bellm LA, Epstein JB, Frame D, Fuchs HJ, Gwede CK, Komaroff E, Nalysnyk L, Zilberberg MD. Mucositis incidence, severity and associated outcomes in patients with head and neck cancer receiving radiotherapy with or without chemotherapy: a systematic literature review. Radiother Oncol. 2003;66(3):253-262.

Vera-Llonch M, Oster G, Hagiwara M, Sonis S. Oral mucositis in patients undergoing radiation treatment for head and neck carcinoma. Cancer. 2006;106(2):329-336.

Zaider M. There is no mechanistic basis for the use of the linear-quadratic expression in cellular survival analysis. Med Phys 1998:25;791-792

FIGURE CAPTIONS

Figure 1: Schematic representation of the cell division cycle: $p\ S(t)$ stem cells enter division at time t; division takes a time τ; during division cells can die with a dying rate γ. At time $t+\tau$ we will have $2p\ S(t)\ \exp(-\gamma\tau)$ exiting the division cycle, of which a fraction $(1-AF)$ will be stem cells and AF will be functional cells.

Figure 2: Schematic representation of the three-compartment model.

Figure 3: Schematic representation of the four-compartment model.

Figure 4: Evolution of densities of cells in the proliferative and functional layers of the skin of mice after irradiation with 13 Gy and 20 Gy – Experimental data (circles with error bars); Best fit obtained with the 3C model (thick solid lines); Best fit ± 1 standard deviation of 1000 simulations considering Gaussian uncertainties with 10% standard deviation around best fitting parameters (thick dashed lines). Thin solid lines show modelling results presented in Dörr and Obeyesekere (2001). Panel A: proliferative layer, 13 Gy; B: proliferative layer, 20 Gy; C: functional layer, 13 Gy; D: functional layer, 20 Gy.

Figure 5: Evolution of densities of cells in the proliferative and functional layers of the skin of mice after irradiation with 13 Gy and 20 Gy – Experimental data (circles with error bars); Best fit obtained with the 4C model (thick solid lines); Best fit ± 1 standard deviation of 1000 simulations considering Gaussian uncertainties with 10% standard deviation around best fitting parameters (thick dashed lines). Thin solid lines show modelling results presented in Dörr and Obeyesekere (2001). Panel A: proliferative layer, 13 Gy; B: proliferative layer, 20 Gy; C: functional layer, 13 Gy; D: functional layer, 20 Gy.

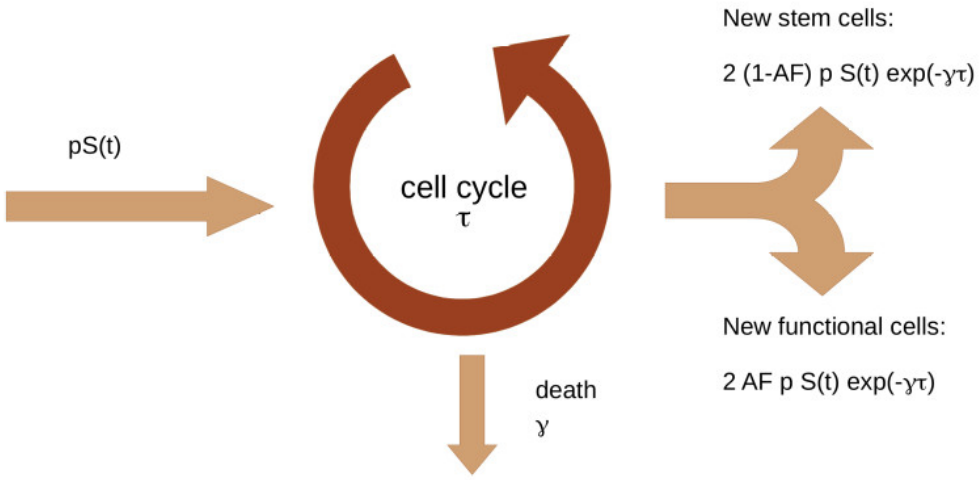

Figure 1: Schematic representation of the cell division cycle: p S(t) stem cells enter division at time t; division takes a time τ; during division cells can die with a dying rate γ. At time t+τ we will have 2p S(t) exp(-γτ) exiting the division cycle, of which a fraction (1-AF) will be stem cells and AF will be functional cells.

64x31mm (300 x 300 DPI)

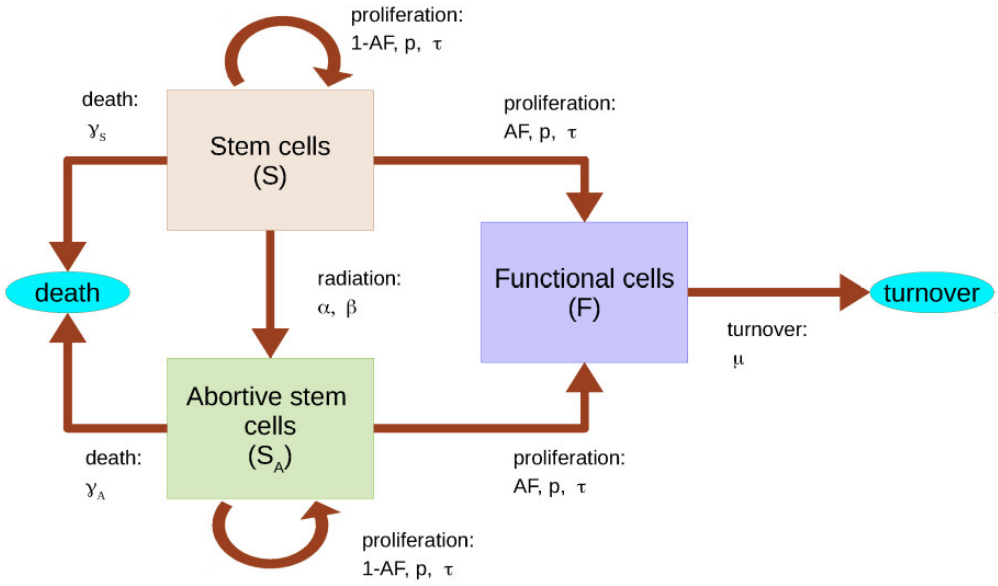

Figure 2: Schematic representation of the three-compartment model.

77x45mm (300 x 300 DPI)

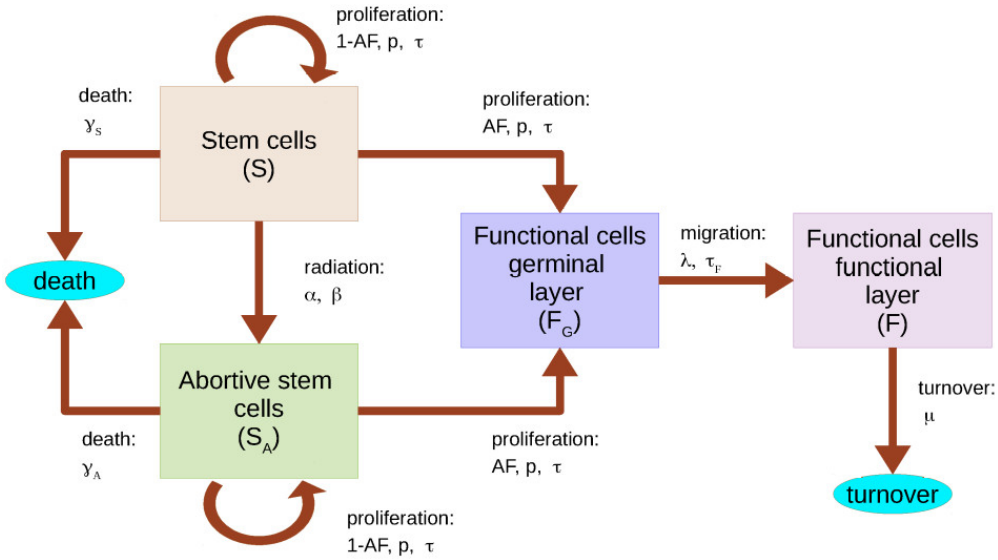

Figure 3: Schematic representation of the four-compartment model.

80x45mm (300 x 300 DPI)

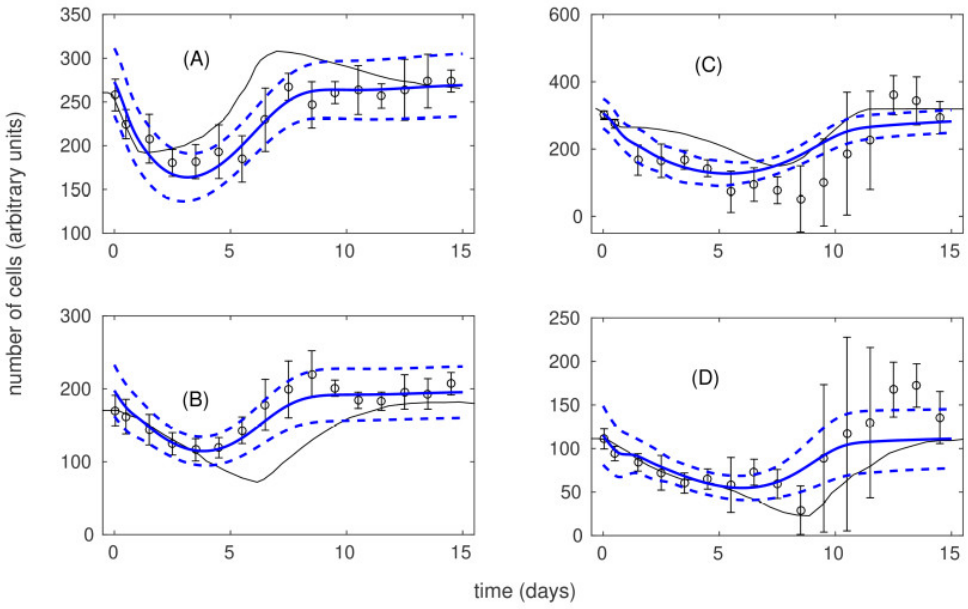

Figure 4: Evolution of densities of cells in the proliferative and functional layers of the skin of mice after irradiation with 13 Gy and 20 Gy – Experimental data (circles with error bars); Best fit obtained with the 3C model (thick solid lines); Best fit ± 1 standard deviation of 1000 simulations considering Gaussian uncertainties with 10% standard deviation around best fitting parameters (thick dashed lines). Thin solid lines show modelling results presented in Dörr and Obeyesekere (2001). Panel A: proliferative layer, 13 Gy; B: proliferative layer, 20 Gy; C: functional layer, 13 Gy; D: functional layer, 20 Gy.

70x43mm (300 x 300 DPI)

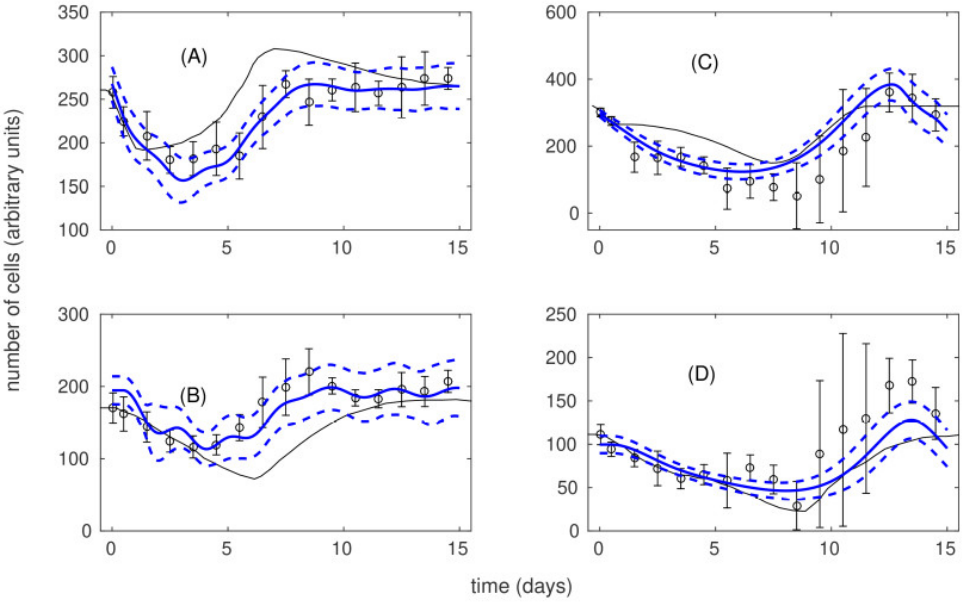

Figure 5: Evolution of densities of cells in the proliferative and functional layers of the skin of mice after irradiation with 13 Gy and 20 Gy – Experimental data (circles with error bars); Best fit obtained with the 4C model (thick solid lines); Best fit ± 1 standard deviation of 1000 simulations considering Gaussian uncertainties with 10% standard deviation around best fitting parameters (thick dashed lines). Thin solid lines show modelling results presented in Dörr and Obeyesekere (2001). Panel A: proliferative layer, 13 Gy; B: proliferative layer, 20 Gy; C: functional layer, 13 Gy; D: functional layer, 20 Gy.

70x43mm (300 x 300 DPI)

Parameter	Definition (Units)	Case 1 (3C)	Case 2 (4C)
τ	Division time (hours)	12	12
γ_S	Death rate of healthy stem cells during mitosis (hours^{-1})	2×10^{-14}	1×10^{-7}
γ_A	Death rate of abortive stem cells during mitosis (hours^{-1})	5.4×10^{-2}	6.2×10^{-2}
μ	Turnover rate of functional cells (hours^{-1})	3.2×10^{-2}	2.3×10^{-2}
α	Linear parameter in LQ model (Gy^{-1})	0.05	0.04
τ_F	Delay in transfer of FCs from proliferative to functional compartments (hours)	-	11
N	Total number of cells	470.6 (13 Gy) 420.3 (20 Gy)	462.3 (13Gy) 397.8 (20 Gy)
f_S	Fraction of stem cells	0.58 (13Gy) 0.73 (20Gy)	0.50 (13 Gy) 0.49 (20 Gy)
f_F	Fraction of functional cells in proliferative compartment	-	0.14 (13Gy) 0.34 (20Gy)
G	Weighted sum of square differences	41.7	36.6
AIC	Akaike information criterion	-7.4	-9.7

Table 1: Best fitting parameters for models 3C and 4C to experimental data reported in Dörr and Obeyesekere (2001), and weighted sum of square differences and Akaike information criterion values for both models.

A mathematical model of dynamics of cell populations in squamous epithelium after irradiation

Martín Parga-Pazos[1,2], Óscar López Pouso[1,2], John D. Fenwick[3,4], Juan Pardo-Montero[1,5,*]

1. Group of Medical Physics and Biomathematics, Instituto de Investigación Sanitaria de Santiago (IDIS), Santiago de Compostela, Spain.

2. Department of Applied Mathematics, Universidade de Santiago de Compostela, Santiago de Compostela, Spain.

3. Department of Molecular and Clinical Cancer Medicine, Institute of Translational Medicine, University of Liverpool, Liverpool, United Kingdom.

4. Department of Physics, Clatterbridge Cancer Centre, Clatterbridge Road, Wirral, United Kingdom.

5. Department of Medical Physics, Complexo Hospitalario Universitario de Santiago de Compostela, Spain.

* Corresponding author

Running title: Model of cell populations in epithelium after irradiation

Corresponding authors: Juan Pardo-Montero, Instituto de Investigación Sanitaria de Santiago (IDIS), Servizo de Radiofísica e Protección Radiolóxica, Hospital Clínico Universitario de Santiago, Trav. Choupana s/n, 15706, Santiago de Compostela; Phone: +34 981950969; E-mail: juan.pardo.montero@sergas.es

Funding details: This project was funded by Instituto de Salud Carlos III (ISCIII) through research grants PI17/01428 and DTS17/00123 (FEDER co-funding). J.P-M. is supported by ISCIII through a Miguel Servet II grant (CPII17/00028, FEDER co-funding). O.L.P. is partially supported by FEDER and Xunta de Galicia (GRC2013-014), and by the Spanish Ministry of Science, Innovation and Universities (MTM2017-86459-R).

Biographical note

Martín Parga-Pazos carried on his MSc thesis in the Group of Medical Physics and Biomathematics at the Health Research Institute of Santiago, working on dynamics of cell populations in squamous epithelium after radiotherapy. He is currently a PhD student at CIC bioGUNE.

Óscar López Pouso is a faculty member in the Department of Applied Mathematics at the University of Santiago de Compostela. His areas of interest are the analysis and numerical resolution of mathematical models for applied sciences and biomedicine.

John D. Fenwick is a senior lecturer in the Institute of Translational Medicine at the University of Liverpool, and honorary consultant clinical scientist at Clatterbridge Cancer Centre, with research interests in radiotherapy and imaging physics.

Juan Pardo-Montero is a "Miguel Servet" scientist at the Health Research Institute of Santiago (Group of Medical Physics and Biomathematics). His current research is focused on biomathematical models in radiotherapy and oncology, and radiation dosimetry.

Abstract

Purpose: To develop multi-compartment mechanistic models of dynamics of stem and functional cell populations in epithelium after irradiation.

Methods and materials: We present two models, with three (3C) and four (4C) compartments respectively. We use delay differential equations, and include accelerated proliferation, loss of division asymmetry, progressive death of abortive stem cells, and turnover of functional cells. The models are used to fit experimental data on the variations of the number of cells in mice mucosa after irradiation with 13 Gy and 20 Gy. Akaike information criteria (AIC) was used to evaluate the performance of each model.

Results: Both 3C and 4C models provide good fits to experimental data for 13 Gy. Fits for 20 Gy are slightly poorer and may be affected by larger uncertainties and fluctuations of experimental data. Best fits are obtained by imposing constraints on the fitting parameters, so to have values that are within experimental ranges. There is some degeneration in the fits, as different sets of parameters provide similarly good fits.

Conclusions: The models provide good fits to experimental data. Mechanistic approaches like this can facilitate the development of mucositis response models to non-standard schedules/treatment combinations not covered by datasets to which phenomenological models have been fitted. Studying the dynamics of cell populations in multifraction treatments, and finding links with induced toxicity, is the next step of this work.

Keywords: biomathematical model, radiotherapy, mucositis, radiobiology

1. Introduction

Intolerable toxicity in *turnover tissues*, like mucosae or skin, is one of the limiting factors of dose escalation and/or treatment shortening in several cancers, especially those of the head-and-neck (Trotti et al. 2003; Vera-Llonch et al. 2006; Russi et al. 2015; Sroussi et al. 2017). Predicting whether different schedules would lead to tolerable or intolerable toxicity is of paramount importance in order to design unconventional radiotherapy schedules that might increase tumor control. Several mathematical models have been developed to explore this issue. Some of these models aim at separating population-wise tolerable and intolerable schedules, like the early model of Fowler et al. (2003), based on the biologically effective dose (BED), later refined by Fenwick et al. (2008), who provided a modified equation for the BED boundary separating tolerable from intolerable schedules. More recently, Strigari et al. (2012) presented a model based on the Lyman-Kutcher-Burman formulation of Normal Tissue Complication Probability. Other models aim at predicting the probability of toxicity of each treated individual, by including individual dose distributions and other patient data and using dose response models, regression, and machine learning techniques (Bhide et al. 2012; Dean et al. 2016a, Dean et al. 2016b, Dean et al. 2017).

All these models are of a phenomenological nature: they do not explore mechanistically what happens to cell populations in tissues, and how that affects toxicity. Even though such phenomenological models find ample application in the clinic due to their specificity, sensitivity, and simplicity (probably rather more application than any mechanistic complex model would find), it is nonetheless of interest to study this problem from a more mechanistic point of view. Such mechanistic approaches can provide useful insight into the problem and can facilitate the development of phenomenological response models to non-standard schedules/treatment combinations not covered by datasets to which the phenomenological models have been fitted.

There exists a large literature on the effect of radiation and fractionation on the populations of cells

in squamous epithelium (Dörr 1997, Dörr 2009, and references therein). However, the mechanistic modeling of what happens to populations of cells in irradiated squamous epithelium has not been fully addressed. Dörr and Obeyesekere (2001) presented a model of this effect. Hanin and Zaider (2013) presented a mechanistic model of radiation-induced damage to normal tissue and its healing kinetic, which is general and not specifically aimed at squamous epithelium. In this work, we present two variations of a multi-compartmental model of cell populations in irradiated epithelium. The model builds on Dörr and Obeyesekere (2001), and it is based on delay differential equations, with delays accounting for cell replication duration, and transfer between compartments. Fenwick (2006) has used delay differential equations to model mucositis, but did not explore the mechanistic origin of such models. The main biological features sustaining the model are based on the *three A's* of repopulation in irradiated squamous epithelium*:* loss of **A**ssymetry, **A**ccelerated proliferation, and **A**bortive divisions (Dörr 1997). Two models are presented, one of them with three compartments: healthy proliferative cells (S), damaged or abortive proliferative cells (S_A), and differentiated functional stem cells (F); the second one with four compartments: S, S_A, functional cells in the proliferative layer (F_G) and functional cells in the functional layer (F). The second model aims at including the particular structure of epithelium, with an inner germinal layer and an outer functional layer.

We analyze the behavior of both models and use them to fit experimental data of cell densities after irradiation in mouse skin.

2. Methods and Materials

2.1. Overview of the models

Our model will include proliferative stem cells (SC) (please notice that by stem cells we refer to cells with proliferation capacity) and fully differentiated, non proliferative, functional cells (FC). In the equilibrium state, under no perturbations like irradiation, SCs will proliferate asymmetrically,

i.e. each SC division will create one SC and one FC. This asymmetric proliferation will keep the population of SCs constant, in its equilibrium value, and will compensate for the natural loss of FC due to tissue turnover.

At any given time, we assume that a fraction p of SCs is proliferating (the rest being quiescent, in the G0 phase). SC division takes a time, τ, and therefore we will explicitly introduce this delay in our model (hence, the need for delay differential equations). During division, SCs may die (due to fatal damage in their DNA or any other problems activating an apoptotic death). We model this probability of death with the parameter γ_S, which controls an exponential death ($dS/dt=-\gamma_S S$). For healthy SC the probability of dying during division will be small, and so will be this parameter. According to this model, if S SCs start division at time t, $2S \exp(-\gamma_S \tau)$ cells will exit the division cycle at time $t+\tau$, of which a fraction $(1-AF)$ will be SCs and AF will be FCs. If division is fully asymmetrical, $AF=0.5$, it will be ½ SCs and ½ FCs. In Figure 1 we show a scheme of the modeling of the division cycle. This model of cell division and death is based on that presented in Mackey et al. (2003).

Irradiation will damage proliferative SCs, turning them into *abortive* stem cells (ACs). The fraction of SCs turning into ACs by the application of a dose d is given by the surviving fraction (SF), calculated according to the linear-quadratic (LQ) model (Fowler 1989), $SF=\exp(-\alpha d-\beta d^2)$, where α and β are the LQ parameters characterizing cell radiosensitivity, which depend on the amount of DNA damage repair and double-strand breaks misrepair (Sachs et al. 1997). There are concerns about the application of the LQ model to high-doses, due to different effects that can impact surviving fractions, like damage saturation of indirect damage effect associated to vascular damage (Brenner 2008, Kirkpatrick et al. 2008). Alternative models have been proposed for high-doses (Guerrero and Li 2004, Hanin and Zaider 2010). In this work, we will rely on the classical LQ model for the sake of simplicity. ACs will still divide, generating new ACs and FCs. However, they

will have a higher probability of death during division, characterized by a parameter γ_A ($\gamma_A >> \gamma_S$). Therefore, ACs will rapidly disappear, causing a shortage of proliferative cells.

Functional cells are considered non-proliferative, and we also assume they do not die due to the application of radiation. This simplification is based on the higher radiosensitivity of proliferating cells in certain phases of the cycle (Pawlik and Keyomarsi 2004). Functional cells will be lost due to natural turnover. This loss is modeled with an exponential (the rate of loss is proportional to the number of cells), with parameter μ.

The rapid disappearance of proliferative cells after irradiation will cause an important perturbation of the equilibrium state: not only will the number of proliferative cells decrease but so will the number of FCs, as newly generated FCs cannot compensate for turnover. The loss of cells triggers accelerated proliferation and loss of asymmetry (Dörr 1997, Trott 1999, Dörr 2009), aiming at compensating for the loss of functional cells and repopulate the compartment of SCs, therefore restoring the equilibrium of the system (if possible). Accelerated proliferation is modeled as an increase of p, the fraction of proliferating SCs (and ACs). Loss of asymmetry is modeled as a decrease of parameter *AF,* therefore resulting in the creation of more proliferative cells per division.

In the first model we include the above mentioned three compartments. Squamous epithelium may present a layered structure, with an inner proliferative layer, where stem cells are located and proliferate, and an outer functional layer, composed of functional cells and subject to turnover. This spatial structure is lost in our model (as spatial coordinates are not considered as in any multi-compartmental model). We have extended our initial model to try to accommodate this layered structure. We assume that the proliferative layer contains both SCs and FCs (we refer to FCs in the proliferative layer as PLFs). The functional layer only contains functional cells (which we refer to as FLFs), which have migrated from the proliferative layer where they were created. We consider

SCs to be present only in the proliferative layer. Division of these SCs will create new PLFs, which will then migrate to the functional layer (this migration in modeled with a rate parameter λ and a delay τ_F). Once in the functional layer, FLFs are subject to turnover, as previously described.

In Figures 2 and 3 we present sketches of the 3-compartment (3C) model and the 4-compartment (4C) model, which graphically illustrate the behavior of both models.

2.2. Case 1: 3-compartments (3C) model

The temporal evolution of the three compartments included in Case 1 (stem cells, *S*, abortive stem cells, S_A, and functional cells, *F*) is described by the following equations:

$$\frac{dS(t)}{dt} = \frac{2p(t-\tau)}{\tau} S(t-\tau) e^{-\gamma_S \tau} (1 - AF) - \frac{p(t)}{\tau} S(t) \quad (1)$$

$$\frac{dS_A(t)}{dt} = \frac{2p(t-\tau)}{\tau} S_A(t-\tau) e^{-\gamma_A \tau} (1 - AF) - \frac{p(t)}{\tau} S_A(t) \quad (2)$$

$$\frac{dF(t)}{dt} = \frac{2p(t-\tau)AF}{\tau} [e^{-\gamma_S \tau} S(t-\tau) + e^{-\gamma_A \tau} S_A(t-\tau)] - \mu F(t) \quad (3)$$

In addition, when radiation is delivered there is an instant transfer of a fraction (1-*SF)* of *S* cells to the abortive stem cell compartment, as previously described. In the above set of equations, *AF* is evaluated at *t*-τ, which is not explicitly included in the equation for the sake of simplicity. The factor *p/τ* can be interpreted as a proliferation rate.

A relationship between *p* and the rest of the parameters can be obtained from the equilibrium state condition (denoted by sub-index 0):

(4)

$$\frac{dF(t)}{dt} = \frac{1}{\tau} p_0 S_0 e^{-\gamma_s \tau} - \mu F_0 = 0 \;\Rightarrow\; p_0 = \frac{\mu \tau F_0}{S_0 e^{-\gamma_s \tau}}$$

As previously described, the parameters *AF* and *p* have a dependence on the number of functional and proliferative cells. It is known that the loss of functional cells triggers accelerated proliferation. In addition, the stem cell compartment will restore itself if damaged (Dörr 1997, Trott 1999). Lacking firm experimental evidence on the functional form of *AF* and *p,* we have considered the following simple expressions for these terms:

$$AF(t) = min\left(0.5, \frac{S(t) + S_A(t)}{S_0}\right) \quad (5)$$

$$p(t) = 1 - (1 - p_0)\frac{F(t)}{F_0} \quad (6)$$

The decrease of proliferative cells will result in a decrease of *AF* and therefore each division will produce on average more proliferative cells (*S* or S_A). On the other hand, *p* will increase with decreasing numbers of functional cells, from a value p_0 at equilibrium to approach 1 when the number of functional cells is very low, which will result in almost 100% of *S* or S_A proliferating.

2.3. Case 2: 4-compartments (4C) model

The temporal evolution of the four compartments included in Case 2 (stem cells, *S*, abortive stem cells, S_A, functional cells in the proliferative layer, F_G, and functional cells in the functional compartment, *F*) is described by the following equations:

$$\frac{dS(t)}{dt} = \frac{2p(t-\tau)}{\tau} S(t-\tau) e^{-\gamma_s \tau}(1 - AF) - \frac{p(t)}{\tau} S(t) \quad (7)$$

$$\frac{dS_A(t)}{dt} = \frac{2\,p(t-\tau)}{\tau} S_A(t-\tau) e^{-\gamma_A \tau}(1-AF) - \frac{p(t)}{\tau} S_A(t) \quad (8)$$

$$\frac{dF_G(t)}{dt} = \frac{2\,p(t-\tau)\,AF}{\tau} [e^{-\gamma_S \tau} S(t-\tau) + e^{-\gamma_A \tau} S_A(t-\tau)] - \lambda F_G(t-\tau_F) \quad (9)$$

$$\frac{dF(t)}{dt} = \lambda F_G(t-\tau_F) - \mu F(t) \quad (10)$$

As previously stated, when radiation is delivered there is an instant transfer of a fraction (1-*SF*) of *S* cells to the abortive stem cell compartment, and *AF* is evaluated at time *t*-*τ*. The following relationships can be obtained from the equilibrium state condition:

$$\frac{dF(t)}{dt} = 0 \;\Rightarrow\; \lambda = \frac{\mu F_0}{F_{G,0}} \quad (11)$$

$$\frac{dF_G(t)}{dt} = 0 \;\Rightarrow\; p_0 = \frac{\lambda \tau F_{G,0}}{S_0 e^{-\gamma_S \tau}} = \frac{\mu \tau F_0}{S_0 e^{-\gamma_S \tau}} \quad (12)$$

Again, sub-indices 0 indicate equilibrium populations. We use the same functional form for *AF* and *p* as in equations (5) and (6).

2.4. Experimental results and fits

We have used our models to fit experimental data reported in Dörr and Obeyesekere (2001). In that article, the authors report variations of numbers of cells (cells/mm) with time in the tongue mucosa of mice after irradiation with 13 Gy and 20 Gy. They include densities of cells in the proliferative layer, functional layer, and total. Data were extracted with the graphical software g3data.

2.5. Numerical implementation

The models were implemented in Matlab (The Mathworks, Natwick, MA), and are solved by employing a Euler method (Press et al. 2017), with a time discretization *Δt*, including some particularities, which are described now: Initial values for each compartment are set in such a way

that we are close to an equilibrium solution. Then, the system evolves without any perturbation (irradiation) so as to achieve a real initial equilibrium state (there may be some shift from the initially set initial values, and some oscillation around new equilibrium values, typical of delay differential equations). When the new equilibrium is achieved (defined as a relative moving average varying less than a given ε) these new values are reset as equilibrium values, and we can start the irradiation phase: the abortive compartment is created at the time of dose delivery and filled with a fraction *SF* of *S* cells.

In addition, a simulated annealing method (Press et al. 2017) was implemented to find best fitting parameters. In order to obtain best fitting parameters, the simulated annealing algorithm can stochastically vary the parameters, but such variations are limited to a range of physically and biologically sound parameters, in order to avoid unreasonable good fits. In order to reduce the number of free parameters, we have imposed α/β=10 in the evaluation of surviving fractions with the LQ model, which is a reasonable value for proliferative cells.

In order to fit the experimental data, we have to obtain numbers of cells in the proliferative and functional layers with our model. In addition to the parameters presented in the differential equations showing the dynamical evolution of each model, we need extra parameters to fit the experimental data. Those parameters are: N_T (overall number of cells pre-irradiation), f_S (fraction of stem cells pre-irradiation), and for the 4C model, f_F (fraction of the total number of functional cells that are in the functional compartment pre-irradiation). From these parameters, we can obtain the values of S_0, and F_0 (and $F_{G,0}$ in the 4C model).

We jointly fit data for 13 Gy and 20 Gy, meaning that the same set of fitting parameters are used for both sets of data, but for N_T, f_F, and f_S. The rationale behind this is that the biological parameters (proliferation, turnover, response to radiation) should be the same in both experiments, but the

number of cells in the proliferative and functional compartments is clearly different in the reported experimental data.

We use the weighted sum of squared differences, G, and the Akaike information criterion, AIC, (Akaike 1974; Gordon 2015) to evaluate the goodness of fits with models 3C and 4C:

$$G=\sum_i \left(\frac{d_{\exp,i}- d_{th,i}}{\sigma_{\exp,i}}\right)^2 \quad (13)$$

$$AIC= 2(k+1)+n\log(G/n) \quad (14)$$

where d_{exp} and d_{th} are experimental and theoretical cell densities, respectively, and σ_{exp} are the experimental uncertainties. On the other hand, k is the number of parameters of the model, and n is the sample size. The 3C model has k=9, the 4C-model k=12, and n=64.

3. Results and discussion

In Figures 4 and 5 we show the evolution of densities of cells in the proliferative and functional layers of the skin of mice after irradiation with 13 Gy and 20 Gy, comparing experimental data and best fits obtained with 3C and 4C models, respectively. We present best fits obtained with our SA algorithm, and we also present an uncertainty analysis to illustrate the effect of uncertainties of parameters in the response of the models: to achieve this we performed 1000 simulations that include perturbation of the best fitting parameters, and report best fits ±1 standard deviation (SD). Uncertainties in the parameters are assumed to follow a normal distribution, with standard deviations of 10% of the mean. Combinations of parameters that were unphysical (e.g. values below 0 or above 100%) or lead to divergences were removed.

Both 3C and 4C models provide a good fit of experimental data for irradiation with 13 Gy

(goodness of fit, G=12.4 and 14.2, respectively). Experimental points are generally within the ±1 SD of the uncertainty analysis, showing that this represents an accurate estimation of experimental uncertainties. On the other hand, fits for 20 Gy are poorer (G=29.2 and 22.5 with 3C and 4C models, respectively). The quality of the fits for 20 Gy may be affected by the larger uncertainty of the experimental data (in fact, the uncertainty analysis with standard deviations of 10% of the mean spans over a range much smaller than the experimental uncertainty bars). Also, the large number of cells in both layers post-recovery, around days 13-15, complicates the fit, as this overgrowth is difficult to fit with our models. It is interesting to hypothesize that the overgrowth might be a result of oscillations in the number of cells around the equilibrium populations. Such behavior can appear in models with delays like those presented in this work, but such a regime has not been fully explored due to the lack of enough experimental data to draw conclusions. Interestingly, the 4C model presents a more oscillatory behavior, which may be due to the presence of more compartments and two delays in the system of differential equations.

We should recall that both 13 Gy and 20 Gy population dynamics have been fitted at once, meaning that the same set of parameters was used for both dose levels (but initial densities of cells, as it is obvious in the experimental data that they differ, see section 2.5). If we allow the optimizer to find different parameters to fit each dose level, the quality of the fit greatly improves, especially for 20 Gy. However, this does not seem justified and should not be the way to proceed in our opinion.

AIC values are similar for the 3C model and the 4C model (-7.5 vs. -9.7), with the larger number of parameters of the 4C model canceling out improved G values. In general, these fits are better than those presented in Dörr and Obeyesekere (2001): better for 13 Gy (G≈14 vs. G≈100) and also for 20 Gy (G≈22 vs. G≈38). When using the Akaike methodology, models with differences in AIC below 2 are generally considered to be equally good, while between 2–6 models are rarely dismissed as differences are not considered significative (Symonds and Moussalli (2011)). Therefore, the two

models can be considered as equally good to fit our dataset.

Best fitting parameters are reported in Table 1. They show a low death rate of healthy stem cells (γ_S~10^{-7} h^{-1}), and a faster a death rate of abortive stem cells (γ_A~0.05 h^{-1}) which results in a half-life of approximately one cell division, and less than 10% of damaged cells undergoing 4 divisions (in line with estimations of around 2-3 abortive divisions per damaged stem cell, Dörr 1997). Turnover rates of functional cells are of the order of 0.03 h^{-1}, resulting in half-lifes of functional cells around 24h. The division time is 12 h, which results in around 28% of the stem cells dividing in the steady state (p_0~0.28). Best fits are obtained with α values around 0.05 Gy^{-1}. While this points to highly radio-resistant cells, it is worth noticing that an even lower value of α (0.02 Gy^{-1}) was used in Dörr and Obeyesekere (2001): cells in this experiment seem to be highly radio-resistant indeed, showing only moderate response to 13 and 20 Gy single-fraction doses. Interestingly, if cells present a decrease in relative radiosensitivity with increasing dose, this would result in a low α value when fitting high-dose data to the LQ model.

It is important to notice that our models present some degeneration: increasing values of α (more radio-sensitive cells) and decreasing values of τ lead to fits of similar quality. This degeneration has not been fully investigated, as the best fitting parameters seem to lack biological meaning (for example equally good fits can be obtained with α = 0.25 Gy^{-1} and τ = 2 h, but such short division times do not seem plausible).

4. Conclusions

Intolerable toxicities in *turnover tissues*, like mucosa or skin, are limiting toxicities in several cancers. Predicting whether a treatment will cause intolerable toxicity is of paramount importance in order to design optimal radiation treatments. Several phenomenological mathematical models have been developed to explore this issue, and some are used in the clinic. It is nonetheless of

interest to study this problem from a more mechanistic point of view.

In this work, we address the modeling of population dynamics of cells in irradiated squamous epithelium. The multi-compartmental models that we have developed intuitively present the underlying biology in mathematical form, in particular the *three A's* of repopulation in irradiated squamous epithelium. While we refer to our model as mechanistic, it is important to point out that the model here presented uses the LQ model to evaluate surviving fractions of irradiated cells. The LQ model was originally introduced as a phenomenological model, and there has been a long-standing debate on the mechanistic origin of the LQ model (Sachs and Brenner 1998, Zaider 1998), which is still active nowadays (Bodgi and Foray 2016). Also, application of the LQ model to large doses per fraction is questioned, but other approaches like the Linear-Quadratic-Linear (LQL) model (Guerrero and Li 2004) could be easily integrated within this methodology.

The models that we present are deterministic models. The experimental data used for validation include relatively large numbers of cells, but when modeling the dynamics of populations of a few cells, stochastic models may be more appropriate (Hanin 2001, Badry and Leder 2016).

The models were used to fit experimental data of cell population dynamics after single dose irradiation, and we obtained good results. Fits obtained with our model are better than those obtained with a model presented by Dörr and Obeyesekere (2001).

Approaches like the one adopted in this work can provide useful insights into the interpretation and development of phenomenological models of toxicity, if toxicity is mainly due to cell loss in the affected organ (Rutkowska et al 2010). In particular, such mechanistic approaches can facilitate the development of response models to non-standard schedules/treatment combinations not covered by datasets to which the phenomenological models have been fitted, like, for example, unconventional

dose fractionations delivering differing doses per week/day. Unconventional chemo-radiotherapy combinations could also be modeled, provided the cytotoxity of chemotherapy is included in the model. Even though we have only fitted single fraction data, the models can also be used for multi-fraction treatments. Studying the dynamics of a cell population in multifraction treatments, and finding links between such dynamics and induced toxicity, is the next step of this work.

Disclosure of interest: The authors report no conflict of interest.

References

Akaike H. A new look at the statistical model identification. IEEE Transactions on Automatic Control. 1974;19(6): 716-723.

Badry H, Leder K. Optimal treatment and stochastic modeling of heterogeneous tumors. Biol Direct. 2016;11:40

Bhide SA, Gulliford S, Schick U, Miah A, Zaidi S, Newbold K, Nutting CM, Harrington KJ. Dose-response analysis of acute oral mucositis and pharyngeal dysphagia in patients receiving induction chemotherapy followed by concomitant chemo-IMRT for head and neck cancer. Radiother Oncol. 2012;103(1):88-91.

Bodgi L, Foray N. The nucleo-shuttling of the ATM protein as a basis for a novel theory of radiation response: resolution of the linear-quadratic model. Int J Radiat Biol 2016:92;117-131

Brenner DJ. The linear-quadratic model is an appropriate methodology for determining isoeffective doses at large doses per fraction. Semin Radiat Oncol 2008:18;234-9.

Dean JA, Wong KH, Welsh LC, Jones AB, Schick U, Newbold KL, Bhide SA, Harrington KJ, Nutting CM, Gulliford SL. Normal tissue complication probability (NTCP) modelling using spatial dose metrics and machine learning methods for severe acute oral mucositis resulting from head and neck radiotherapy. Radiother Oncol. 2016;120(1):21-27.

Dean JA, Wong KH, Gay H, Welsh LC, Jones AB, Schick U, Oh JH, Apte A, Newbold KL, Bhide SA, Harrington KJ, Deasy JO, Nutting CM, Gulliford SL. Functional data analysis applied to modeling of severe acute mucositis and dysphagia resulting from head and neck radiation therapy. Int J Radiat Oncol Biol Phys. 2016;96(4):820-831.

Dean JA, Welsh LC, Wong KH, Aleksic A, Dunne E, Islam MR, Patel A, Patel P, Petkar I, Phillips I, Sham J, Schick U,

Newbold KL, Bhide SA, Harrington KJ, Nutting CM, Gulliford SL. Normal Tissue Complication Probability (NTCP) modelling of severe acute mucositis using a novel oral mucosal surface organ at risk. Clin Oncol (R Coll Radiol). 2017;29(4):263-273.

Dörr W. Three A's of repopulation during fractionated irradiation of squamous epithelia: Asymmetry loss, Acceleration of stem-cell divisions and Abortive divisions. Int J Radiat Biol. 1997;72(6):635-643

Dörr, W. Time factors in normal tissue responses to irradiation. In: Basic Clinical Radiobiology. (Eds. M. Joiner, A. Vander Kogel), pp.149–157, Hodder Arnold, London, 2009.

Dörr W, Obeyesekere MN. A mathematical model for cell density and proliferation in squamous epithelium after single-dose irradiation. Int J Radiat Biol. 2001;77(4):497-505.

Fenwick JD. Delay differential equations and the dose-time dependence of early radiotherapy reactions. Med Phys. 2006;33(9):3526-3540.

Fenwick JD, Lawrence GP, Malik Z, Nahum AE, Mayles WP. Early mucosal reactions during and after head-and-neck radiotherapy: dependence of treatment tolerance on radiation dose and schedule duration. Int J Radiat Oncol Biol Phys. 2008;71(2):625-634.

Fowler JF. The linear-quadratic formula and progress in fractionated radiotherapy. Br J Radiol. 1989 ;62(740):679-94

Fowler JF, Harari PM, Leborgne F, Leborgne JH. Acute radiation reactions in oral and pharyngeal mucosa: tolerable levels in altered fractionation schedules. Radiother Oncol. 2003;69(2):161-168.

Gordon RA. Regression Analysis for the Social Sciences, Routledge 2015.

Guerrero M, Li XA. Extending the linear- quadratic model for large fraction doses pertinent to stereotactic radiotherapy. Phys Med Biol 2004;49:4825-4835.

Hanin LG. Iterated birth and death process as a model of radiation cell survival. Math Biosci. 2001;169:89-107.

Hanin LG, Zaider M. Cell-survival probability at large doses: an alternative to the linear-quadratic model. Phys Med Biol. 2010;55(16):4687-7702.

Hanin L, Zaider M. A mechanistic description of radiation-induced damage to normal tissue and its healing kinetics.

Phys Med Biol. 2013;58:825-839.

Kirkpatrick JP, Meyer JJ, Marks LB. The linear-quadratic model is inappropriate to model high dose per fraction effects in radiosurgery. Semin Radiat Oncol 2008:18;240-3.

Mackey MC, Haurie C, Bélair J. Cell replication and control. In Non linear dynamics in physiology and medicine (Eds. A. Beuter, L Glass, MC Mackey, MS Titcombe), pp 233-269, Springer 2003.

Pawlik TM, Keyomarsi K. Role of cell cycle in mediating sensitivity to radiotherapy. Int J Radiat Oncol Biol Phys. 2004;59(4):928-42.

Press WH, Teukolsky SA, Vetterling WT, Flannery BP. Numerical Recipes: The Art of Scientific Computing, Cambridge University Press 2007.

Rutkowska E, Baker C, Nahum A. Mechanistic simulation of normal-tissue damage in radiotherapy - implications for dose-volume analyses. Phys Med Biol 2010;55:2121-36.

Russi EG, Moretto F, Rampino M, Benasso M, Bacigalupo A, De Sanctis V, Numico G, Bossi P, Buglione M, Lombardo A, Airoldi M, Merlano MC, Licitra L, Denaro N, Pergolizzi S, Pinto C, Bensadoun RJ, Girolomoni G, Langendijk JA. Acute skin toxicity management in head and neck cancer patients treated with radiotherapy and chemotherapy or EGFR inhibitors: Literature review and consensus. Crit Rev Oncol Hematol. 2015;96(1):167-182.

Sachs RK, Hahnfeld P, Brenner DJ. The link between low-LET dose-response relations and the underlying kinetics of damage production/repair/misrepair. Int J Radiat Biol 1997;72:351-374

Sachs RK, Brenner DJ. The mechanistic basis of the linear-quadratic formalism. Med Phys 1998:25;2071-2072

Sroussi HY, Epstein JB, Bensadoun RJ, Saunders DP, Lalla RV, Migliorati CA, Heaivilin N, Zumsteg ZS. Common oral complications of head and neck cancer radiation therapy: mucositis, infections, saliva change, fibrosis, sensory dysfunctions, dental caries, periodontal disease, and osteoradionecrosis. Cancer Med. 2017;6(12):2918-2931.

Strigari L, Pedicini P, D'Andrea M, Pinnarò P, Marucci L, Giordano C, Benassi M. A new model for predicting acute mucosal toxicity in head-and-neck cancer patients undergoing radiotherapy with altered schedules. Int J Radiat Oncol Biol Phys. 2012;83(5):e697-702.

Symonds MR, Moussalli A. A brief guide to model selection, multimodel inference and model averaging in behavioural

ecology using Akaike's information criterion. Behav Ecol Sociobiol 2011;65(1):13-21.

Trott KR. The mechanisms of acceleration of repopulation in squamous epithelia during daily irradiation. Acta Oncologica. 1999;38:153-157

Trotti A, Bellm LA, Epstein JB, Frame D, Fuchs HJ, Gwede CK, Komaroff E, Nalysnyk L, Zilberberg MD. Mucositis incidence, severity and associated outcomes in patients with head and neck cancer receiving radiotherapy with or without chemotherapy: a systematic literature review. Radiother Oncol. 2003;66(3):253-262.

Vera-Llonch M, Oster G, Hagiwara M, Sonis S. Oral mucositis in patients undergoing radiation treatment for head and neck carcinoma. Cancer. 2006;106(2):329-336.

Zaider M. There is no mechanistic basis for the use of the linear-quadratic expression in cellular survival analysis. Med Phys 1998:25;791-792

FIGURE CAPTIONS

Figure 1: Schematic representation of the cell division cycle: $p\ S(t)$ stem cells enter division at time t; division takes a time τ; during division cells can die with a dying rate γ. At time $t+\tau$ we will have $2p\ S(t)\ \exp(-\gamma\tau)$ exiting the division cycle, of which a fraction $(1-AF)$ will be stem cells and AF will be functional cells.

Figure 2: Schematic representation of the three-compartment model.

Figure 3: Schematic representation of the four-compartment model.

Figure 4: Evolution of densities of cells in the proliferative and functional layers of the skin of mice after irradiation with 13 Gy and 20 Gy – Experimental data (circles with error bars); Best fit obtained with the 3C model (thick solid lines); Best fit ± 1 standard deviation of 1000 simulations considering Gaussian uncertainties with 10% standard deviation around best fitting parameters (thick dashed lines). Thin solid lines show modelling results presented in Dörr and Obeyesekere (2001). Panel A: proliferative layer, 13 Gy; B: proliferative layer, 20 Gy; C: functional layer, 13 Gy; D: functional layer, 20 Gy.

Figure 5: Evolution of densities of cells in the proliferative and functional layers of the skin of mice after irradiation with 13 Gy and 20 Gy – Experimental data (circles with error bars); Best fit obtained with the 4C model (thick solid lines); Best fit ± 1 standard deviation of 1000 simulations considering Gaussian uncertainties with 10% standard deviation around best fitting parameters (thick dashed lines). Thin solid lines show modelling results presented in Dörr and Obeyesekere (2001). Panel A: proliferative layer, 13 Gy; B: proliferative layer, 20 Gy; C: functional layer, 13 Gy; D: functional layer, 20 Gy.